Impact of assimilating spaceborne microwave signals for improving hydrological prediction in ungauged basins

Yu Zhang[1, 2,5], Yang Hong[1, 2, 3,5], Jonathan J. Gourley[4], XuGuang Wang[5, 6], G. Robert Brakenridge[7], Tom De Groeve[8] and Humberto Vergara[1, 2]

[1]School of Civil Engineering and Environmental Science, University of Oklahoma, OK, USA

[2]Advanced Radar Research Center, University of Oklahoma, Norman, OK, USA

[3]Water Technology for Emerging Region (WaTER) Center, University of Oklahoma, OK USA

[4]NOAA/National Severe Storms Laboratory, Norman, OK, USA

[5]Center for Analysis and Prediction of Storms, University of Oklahoma, Norman, OK, USA

[6]School of Meteorology, University of Oklahoma, OK, USA

[7]CSDMS, INSTAAR, University of Colorado. Boulder, CO, USA

[8] Joint Research Centre of the European Commission, Ispra, Italy

May 2013

**Corresponding author address:*

Dr. Yang Hong

National Weather Center ARRC Suite 4610, 120 David L. Boren Blvd., Norman, OK 73072 USA

Tel: 405-325-3644; Fax: 405-325-4217; email: yanghong@ou.edu; web: http://hydro.ou.edu

Abstract

The availability of in-situ data has been a constraining issue in hydrological prediction, especially in those regions that are only sparsely monitored or completely ungauged. The application of remote-sensing data, without conventional in-situ hydrological measurements, to force, calibrate and update a hydrologic model is a major contribution of this study. First, a rainfall-runoff hydrological model called CREST, coupled with EnSRF, is used for exceedance probability-based flood prediction. Then, this advanced flood-prediction framework, with different experimental designs, is forced by TRMM precipitation while Aqua AMSR-E microwave brightness temperature signals is used for model calibration and data assimilation for progressively improved river discharge prediction. Results indicate that solely relying on remote-sensing data for model forcing, parameter calibration, and state updating with EnSRF, the designed framework can adequately predict flooding events. A high flow threshold was applied and has further improved modeling performance, particularly in the flooding seasons, with a flood warning lead-time of one day. Given the anticipated global availability of satellite-based precipitation (i.e. GPM) and AMSR-E like passive microwave signal information (i.e. SMAP) in near real-time, this proposed research framework could potentially contribute to the exceedance probability-based flood prediction in the vast sparsely gauged or ungauged basins around the world.

1. Introduction

Insufficient ground gauge observations have been historical barriers in hydrological predictions. Over the globe, especially in Africa, it is much more common for a given basin to be only sparsely or not monitored at all by in-situ observation networks. However, recent advancement in satellite remote-sensing technology bears the promising potential to overcome the limited spatial coverage of in-situ observation networks, thus providing the potential for hydrological predictions by being creatively used as the forcing (e.g. satellite precipitation estimation), calibration basis (e.g. passive microwave streamflow signal), and sources for assimilation (e.g. satellite-detected soil moisture estimation and passive microwave streamflow signals). This forecast system based entirely on remote-sensing information thus enhances the reliability of streamflow prediction in poorly-gauged basins, and makes streamflow prediction possible even in ungauged basins.

Considering hydrological modeling in those basins with limited ground surface observation networks, a great deal of success has been achieved through the recent availability of remote-sensing precipitation data (e.g. [*Hong et al.*, 2004; *Huffman et al.*, 2007; *Joyce et al.*, 2004; *Sorooshian et al.*, 2000; *Turk and Miller*, 2005]). Besides utilizing the remote-sensing precipitation data as forcing, remote-sensing soil moisture data can also facilitate hydrological prediction by data assimilation approaches (e.g. [*Crow and Ryu*, 2009; *Crow et al.*, 2005; *Gao et al.*, 2007; *V Pauwels et al.*, 2002]). A number of studies have shown improved accuracy by calibrating hydrologic models and through assimilating in-situ soil moisture observations and gauge-based streamflow measurements into hydrological models. (e.g. [*Aubert et al.*, 2003; *Clark et al.*, 2008; *V R Pauwels and De Lannoy*, 2006]). The use of streamflow estimates from remote-sensing methods is a new area being explored, also for model calibration and data assimilation. Recently, the Global Flood Detection System (GFDS, http://www.gdacs.org/flooddetection/), began using a passive microwave sensor, AMSR-E, together with the Tropical Rainfall Measurement Mission (TRMM) Microwave Imager (TMI), to measure surface brightness temperatures, which can be used creatively to infer streamflow and thus show the potential to monitor floods over the globe [*Brakenridge et al.*, 2007]. While prior studies have evaluated the potential application of the AMSR-E sensor for discharge estimation and flood detection [*Salvia et al.*, 2011; *Temimi et al.*, 2007; *Temimi et al.*, 2011], they all required in-situ streamflow information. In this study, the passive microwave streamflow signals are utilized directly, without in-situ streamflow observations, in a hydrologic model to calibrate the hydrological model first; then the frequency (exceedance probability) of the remote-sensing streamflow signals is assimilated into the hydrological model in order to demonstrate probabilistic flood prediction for an African basin.

2. Study Basin, Data Sources and Methodology

2.1 Study Basin

The Okavango River, which runs for about 1100 km from central Angola and flows through Namibia and Botswana, is the fourth longest river in southern Africa (Figure 1.). The Okavango catchment is approximately 413,000 km^2; it originates in the headwaters of central Angola, then the Cubango and Cuito tributaries meet to form the Cubango-Okavango River near the border of Angola and Namibia and flow into the Okavango Delta in Botswana. The upper stream region belongs in a subtropical climate zone with annual precipitation around 1300mm while the downstream region, which contains the Kalahari Desert, belongs to the semi-arid climate zone with annual precipitation around 450mm [*D A Hughes et al.*, 2006; *Christian Milzow et al.*, 2009a]. The headwater region, which is the northern part of the basin, is mainly covered by the ferralsols soil with a lower hydraulic conductivity. The headwater region also has a high forest cover and contributes significantly to the river runoff [*D A Hughes et al.*, 2006]. The rest of the basin is dominated by arenosals soil (www.sharing-water.net), which is very porous with high hydraulic conductivity, so that water drains rapidly, leaving little moisture for plants. As mentioned by [*D A Hughes et al.*, 2006], around 95% of inflow is lost in the atmosphere due to high potential evapotranspiration rate and only a small portion contributes to groundwater.

Several studies in the Okavango River Basin have investigated the hydrological response under climate change [*Andersson et al.*, 2006; *D Hughes et al.*, 2011; *D A Hughes et al.*, 2006; *McCarthy et al.*, 2003; *Christian Milzow et al.*, 2009b]. Since the Okavango River basin is one of the most important economic and water resources in southern Africa, additional studies have been solicited to assist in the decision-making for water management in this basin. The main tributary of Okavango River - the Cubango River, which is mainly located in Angola, is selected as the study basin. It accounts for a majority of the available water resources in the Okavango river. The Rundu gauge station is the outlet of the Cubango River; at Rundu Gauge, both gauge-based streamflow and the remote-sensing discharge estimates (i.e., the AMSR-E & TMI streamflow signals) are available.

2.2 Data Sources

This study develops an advanced exceedance probability-based, flood-prediction framework, which is based entirely on satellite remote-sensing data without a requirement of conventional in-situ hydrological measurements. The in-situ streamflow observation is only used in this study to evaluate the exceedance probability-based hydrological prediction algorithm. The proposed data sets that were applied in this study include:

- TRMM RT Satellite Precipitation Estimates

Tropical Rainfall Measuring Mission (TRMM) satellite precipitation estimation is taken as an alternative forcing data into hydrological modeling in this study since the Okavango River Basin is poorly gauged [*C. Milzow et al.*, 2011]. TRMM Multi-satellite Precipitation Analysis (TMPA) provides two standard 3B42-level products: the near-real-time 3B42 RT which uses the TRMM combined instrument dataset to calibrate the data and the post-real-time research product 3B42 V7 (level 7) which adjusts the rainfall accumulation by gauge analysis [*Huffman et al.*, 2007]. Both 3B42 RT and 3B42 V7 products are quasi-global with coverage from 50 °N to 50 °S latitude. In this study, the TRMM 3B42 RT with a spatial resolution of 0.25 ° (approximate to 25km in the tropical area) and temporal resolution of three hourly, is processed into daily accumulations as well as basin averages and applied as the forcing data to drive the hydrological model.

- FEWS PET

PET (Potential Evapotranspiration) comes from the Famine Early Warning System Network (FEWS NET; http://igskmncnwb015.cr.usgs.gov/Global/) with a spatial resolution of 0.25 °, and is likewise processed into daily and basin averages as additional forcing to the model.

- The Passive Microwave Streamflow signal from TRMM and Aqua

The Global Flood Detection System uses near-real-time, satellite-based, remote-sensing data to monitor floods over the globe. In this system, a passive microwave sensor, AMSR-E, together with TRMM TMI (TRMM Microwave Imager) sensor, is used to measure the brightness temperature at 36.5GHz, descending orbit with horizontal polarization, which responds to surface wetness and thus flooding [*Brakenridge et al.*, 2007]. A wet pixel (usually over the surface of a river) is selected to measure the brightness temperature of the measurement (M) area while an adjacent dry pixel is selected to measure the brightness temperature of the calibration (C) area (usually over the land near the wet pixel); the ratio of the measurement and calibration brightness temperature is referred as the streamflow signal (Eq. (1)).

- $$M / C\ Ratio = Tb_m / Tb_c \quad (1)$$

The main merit of the AMSR-E passive microwave sensor onboard the NASA EOS Aqua satellite is that it is not restricted by cloud cover and provides data availability for daily flood monitoring over the globe. For further detailed information regarding the GFDS streamflow signals, please refer to [*Brakenridge et al.*, 2007; *Kugler and Groeve*, 2007].

- Ground-based streamflow observation

Besides the passive microwave streamflow signal data at Rundu for both calibration and assimilation (will be specified in 2.5 Experiment design), ground-based streamflow observation at Rundu, Namibia, was used to evaluate the performance of the proposed "exceedance probability based flood-prediction framework" [*Khan et al.*, 2012] in an upstream catchment – Cubango of around 95000km^2

2.3 Model

In this study, a simplified and lumped version of the CREST (**C**oupled **R**outing and **E**xcess **ST**orage , [*Wang et al.*, 2011]) was applied, together with the satellite data and the EnSRF (Ensemble Square Root Filter) data assimilation approach, to provide exceedance probability-based hydrological predictions over the Cubango basin. The model structure is shown by Figure 2: following the forcing data of precipitation and potential evapotranspiration, there is one excess storage reservoir by the vegetation canopy and three surface water excess storage reservoirs representing the three underlying soil layers. Then, the flow into each of three overland flow linear reservoirs and one interflow reservoir is governed by the overland reservoir discharge multiplier LEAKO and the interflow reservoir discharge multiplier LEAKI.

2.4 EnSRF

A sequential data assimilation technique - Ensemble Square Root Filter (EnSRF), is applied to assimilate passive microwave streamflow signals into CREST. Unlike the traditional EnKF which requires perturbing both forcing data and observations, the EnSRF only perturbs the forcing data and the ensemble mean is updated by the observation. [*Whitaker and Hamill*, 2002] demonstrated that there is no additional computational cost by EnSRF relative to EnKF, and EnSRF performs more accurately than EnKF for the same ensemble size. But it still remains a research topic to compare the accuracy and efficiency of different sequential data assimilation approaches (e.g. EnKF, EnSRF). The major equations of EnSRF are listed below:

$$X^a = X^b + \hat{K}(y - H(X^b)) \quad (2)$$

X^a is the updated estimate of the analyzed state ($n \times 1$ dimension and n is the number of ensembles);

X^b is the background model forecast, which is also referred to the first guess in data assimilation ($n \times 1$ dimension);

y is the observation ($p \times 1$ dimension and p is the number of observations), which is the streamflow measurements in this study;

H is the observation operator that converts the states in the model into observation space ($p \times n$ dimension);

$\hat{K}$ refers to the traditional Kalman gain.

Let's denote the ensemble X^b as

$$X^b = (x_1^b, x_2^b, \ldots, x_n^b) \quad (3)$$

Where we ignore time index and the subscript represents the ensemble member. The ensemble mean is then defined as

$$\overline{X^b} = \frac{1}{n}\sum_{i=1}^{n} x_i^b \tag{4}$$

The perturbation from the mean for the i th member is

$$x_i'^b = x_i^b - \overline{x^b} \tag{5}$$

Then X'^b is defined as a matrix formed from the ensemble of perturbations:

$$X'^b = (x_1'^b, x_2'^b, \dots, x_n'^b) \tag{6}$$

An estimation of background error covariance is defined as

$$\hat{P}^b = \frac{1}{n-1} X'^b (X'^b)^T \tag{7}$$

However, in practice, we do not calculate $\hat{P}^b$, but rather calculate $\widehat{\mathrm{P}}^{\mathrm{b}}\mathrm{H}^{\mathrm{T}}$ and $\mathrm{H}\widehat{\mathrm{P}}^{\mathrm{b}}\mathrm{H}^{\mathrm{T}}$ are evaluated by the following equations:

$$\widehat{\mathrm{P}}^{\mathrm{b}}\mathrm{H}^{\mathrm{T}} = \frac{1}{\mathrm{m}-1}\sum_{i=1}^{m}(\mathrm{X}_{\mathrm{i}}^{\mathrm{b}} - \overline{\mathrm{X}}^{\mathrm{b}})(\mathrm{H}(\mathrm{X}_{\mathrm{i}}^{\mathrm{b}} - \overline{\mathrm{H}(\mathrm{X}^{\mathrm{b}})}))^{\mathrm{T}} \tag{8}$$

$$\mathrm{H}\widehat{\mathrm{P}}^{\mathrm{b}}\mathrm{H}^{\mathrm{T}} = \frac{1}{\mathrm{m}-1}\sum_{i=1}^{m}(\mathrm{H}(\mathrm{X}_{\mathrm{i}}^{\mathrm{b}}) - \mathrm{H}(\overline{\mathrm{X}}^{\mathrm{b}}))(\mathrm{H}(\mathrm{X}_{\mathrm{i}}^{\mathrm{b}} - \overline{\mathrm{H}(\mathrm{X}^{\mathrm{b}})}))^{\mathrm{T}} \tag{9}$$

Here, m is the ensemble size. Then the traditional Kalman gain $\widehat{\mathrm{K}}$ can be calculated by Eq (10),

$$\widehat{\mathrm{K}} = \widehat{\mathrm{P}}^{\mathrm{b}}\mathrm{H}^{\mathrm{T}}(\mathrm{H}\widehat{\mathrm{P}}^{\mathrm{b}}\mathrm{H}^{\mathrm{T}} + \mathrm{R})^{-1} \tag{10}$$

R is the observation error covariance with a dimension of $p \times p$. In EnSRF, the reduced Kalman gain $\widetilde{\mathrm{K}}$ is used to update the deviation from the ensemble mean as estimated by the following equation,

$$\widetilde{\mathrm{K}} = \left(1 + \sqrt{\frac{\mathrm{R}}{\mathrm{H}\widehat{\mathrm{P}}^{\mathrm{b}}\mathrm{H}^{\mathrm{T}} + \mathrm{R}}}\right)^{-1}\widehat{\mathrm{K}} \tag{11}$$

The ensemble mean can be updated by

$$\overline{\mathrm{X}}_{\mathrm{i}}^{\mathrm{a}} = \overline{\mathrm{X}}_{\mathrm{i}}^{\mathrm{b}} + \widehat{\mathrm{K}}(\mathrm{y} - \mathrm{H}(\overline{\mathrm{X}}_{\mathrm{i}}^{\mathrm{b}})) \tag{12}$$

The perturbation (deviation of ensemble mean) can be updated by

$$X_i'^a = X_i'^b - \widetilde{K}H(X_i'^b) \quad (13)$$

The final analysis follows as

$$X_i^a = \overline{X}_i^a + X_i'^a \quad (14)$$

As mentioned above, when the EnSRF is applied, the forcing data (which is the precipitation in this study) needs to be perturbed. Precipitation perturbations in this study are defined as

$$P_i = P + \varepsilon_i \quad (15)$$

where ε_i is a random noise factor drawn from a Gaussian distribution

$$\varepsilon_i \sim N(0, R) \quad (16)$$

At each time step, an independent rainfall error is generated by Gaussian distribution (refer to eq. (15) and (16)) and added to the original basin average precipitation.

2.5 Experimental design

The C/M radiance ratio, which is the reciprocal of M/C ratio signal (e.q. (1)), is correlated at a significant level with observed streamflow especially during the peak flow periods, as shown in Figure 3. Based on the high correlation coefficient between the gauge-based streamflow and the C/M radiance ratio, an innovative calibration method – the flood frequency approach, was proposed by [*Khan et al.*, 2012], which first requires the conversion of model-simulated streamflow into exceedance probability, and then takes “max(CC)” as the objective function to conduct the automatic hydrological calibration via the algorithm Shuffled Complex Evolution – University of Arizona (SCE-UA, [*Duan et al.*, 1994]). The flood frequency approach utilizes the period of recorded observations to compute the frequency or exceedance probability. This approach essentially normalizes the streamflow observations from absolute units ($m^3\ s^{-1}$) to dimensionless values in the frequency domain. The same approach can be applied to any time series data (i.e., passive microwave streamflow signal) as long as there is a sufficiently long record to represent climatological conditions and the signal is temporally correlated to streamflow.

As shown by Table 1, experiment 1, which was conducted in absolute streamflow units ($m^3 s^{-1}$), is the traditional gauged-based approach to model calibration and data assimilation. It sets the reference to be compared to the frequency-based, remote-sensing approaches in Experiment 2. Experiment 2 represents the advanced exceedance probability-based streamflow prediction framework; in Experiment 2, the passive microwave streamflow C/M radiance ratio at Rundu gauge was first used to automatically calibrate the model parameters as in Experiment 1, but using the flood frequency approach described in [*Khan et al.*, 2012], and then the signal frequency was assimilated into CREST model via EnSRF.

3 Results and Discussion

Experiment 1 is the reference experiment; the model was calibrated by gauge-based streamflow observations for the period 2003 to 2005 with a computed RMSE of 34% and NSCE of 0.88. Then, the model was validated for the period 2006 to 2007, in which the RMSE shot up to 64% and the NSCE dropped to 0.33. In order to enhance the hydrological performance, the gauge streamflow observation was assimilated into the well-calibrated lumped CREST model via EnSRF at daily time step. After assimilation, the modeling performance was improved significantly during both calibration and validation periods. (Note: the statistical evaluation excludes the first half-year due to the bad first guesses at the beginning for each experiment.) The two simulations illustrated in Figure 4 serve as the stream gauge-based reference for the Open Loop and Assimilation experiments focused on the use of the microwave streamflow signals hereafter.

Figure 3 shows the time series of the passive microwave C/M radiance ratio (green line), which is used as the streamflow proxy for automatically estimating the model parameters. The C/M radiance ratio matches well with the gauge streamflow observations during the high flow period, but shows noise during the low flow period because of the insensitivity of the AMSR-E and TMI sensors to low flows. In Experiment 2(a), the sources of data for model calibration are the C/M radiance ratios, but the simulated and observed streamflow data have been converted into the frequency domain and expressed as the exceedance probability (Figure. 5a). This conversion degraded the skill of the Open Loop simulation compared to the one in Experiment 1 during the calibration period, but enhanced the Open Loop simulation during the validation period with NSCE increased from 0.33 to 0.81. After assimilation, the streamflow signal indicates a small peak near Nov 2003 that was not observed by the stream gauge (Figure .5(a)). This error was not reflected in the Open Loop simulation; however, by assimilating the C/M radiance ratio with noise into the model during the low flows, errors during low flows result. The performance of the simulations was poor for low flows, but remarkable for high flows. This latter feature prompted us to devise Experiment 2(b) the same as the Assimilation component of Experiment 2(a), but the radiance ratio data are assimilated only if the exceedance probability is < 30%. In other words, the C/M radiance ratio data are trusted only during high flow conditions. After application of this subjectively chosen threshold, the red curve in Figure. 5b illustrates very similar performance during high flows as in Experiment 2(a) (red curve in Figure. 5a), but the prior problems during low flows have been alleviated. The RMSE (26% during calibration period and 23% during validation period) is even better than the reference simulations in Experiment 1 that assimilated gauge streamflow (in absolute units). The NSCE of 0.79 and 0.84 during calibration and validation periods, respectively, is only a slight reduction from the reference values. Nonetheless, this reduction is quite modest considering Experiment 2b is based entirely on remote-sensing data.

Overall, the lumped CREST coupled with state estimation through an EnSRF approach can effectively improve flood prediction using remote-sensing data alone in the Cubango river basin. A limitation, as mentioned by [*Khan et al.*, 2012] is that the use of AMSR-E signals for streamflow estimation is limited to medium- and large-scale basins. Moreover, the signal was found to be uncorrelated with observed streamflow during low flow periods. These constraints must be considered when using the GFDS streamflow signals to infer streamflow for hydrologic model calibration and state estimation.

4 Conclusion

The application of remote-sensing data, alone, to force, calibrate and update a hydrologic model is a major contribution of this study. More generally, the approach developed and benchmarked herein can have great potential for predicting floods for the vast number of river basins throughout the world that are poorly gauged or even ungauged. In the Cubango River basin, data from an in-situ streamflow gauge was used for model calibration and data assimilation in a traditional manner, providing a benchmark for evaluating the use of the passive microwave sensor-derived streamflow signals as a proxy for streamflow. Then, the passive microwave streamflow signals were converted into exceedance probability; i.e., in the frequency domain, to be applied similarly as the traditional approach for calibration and assimilation.

The major outcomes from this study are summarized as follows:

- In the absence of data assimilation (i.e., Open Loop), model performance was limited due to the inherent deficiencies of the model structure, but was more likely dominated by bias in the rainfall forcing from the TRMM 3B42RT algorithm.
- The implementation of the EnSRF in all experiments resulted in a significant improvement over the Open Loop simulations except Experiment 2(a).
- When the GFDS streamflow signals converted to the frequency domain were substituted as the streamflow proxy for the Open Loop simulation in Experiment 2(a), there was a significant reduction in model skill compared to using gauged streamflow during the calibration period, but there was a significant enhancement during the validation period. However, the assimilation of the GFDS signals during the calibration period degraded the RMSE to 36% (from 27% for Open Loop) and the NSCE to 0.61 (from 0.77 for Open Loop), which was worse than the values in the reference Experiment 1. This characteristic was found to be a result of poor sensitivity of the GFDS signal during low flow periods.
- The final Experiment 2(b) assimilated the AMSR-E signal only if the exceedance probability was < 30%; i.e., during high flow periods. The application of this threshold resulted in model skill that was comparable to what was obtained in the reference Experiment 1.

Given the real-time availability of satellite-based precipitation and AMSR-E and TMI-like passive microwave streamflow signal information, we argue that this work contributes to the decadal initiative of prediction in ungauged basins. Moreover, this study presents a potential paradigm shift in the use of streamflow exceedance probabilities, different from traditional methods reliant on in-situ streamflow observation for calibration, and towards new techniques and new types of observations. These observations and new methods are particularly imperative for the vast sparsely gauged or ungauged basins around the world. More promisingly, assimilation of remote-sensing information for improving hydrological prediction can be increasingly appreciated and supported by the current TRMM and anticipated GPM (Global Precipitation Mission, to be launched in earlier 2014), together with the future SMAP (Soil Moisture Active and Passive, to be launched in 2014). Both missions are anticipated to provide better precipitation and surface wetness estimates in terms of coverage, accuracy, and resolutions, which bears promise to further improve flood predictions in combination with the proposed framework in this study.

References:

Andersson, L., J. Wilk, M. C. Todd, D. A. Hughes, A. Earle, D. Kniveton, R. Layberry, and H. H. Savenije (2006), Impact of climate change and development scenarios on flow patterns in the Okavango River, *Journal of Hydrology*, *331*(1), 43-57.

Aubert, D., C. Loumagne, and L. Oudin (2003), Sequential assimilation of soil moisture and streamflow data in a conceptual rainfall–runoff model, *Journal of Hydrology*, *280*(1), 145-161.

Brakenridge, G. R., S. V. Nghiem, E. Anderson, and R. Mic (2007), Orbital microwave measurement of river discharge and ice status, *Water Resources Research*, *43*(4), W04405.

Clark, M. P., D. E. Rupp, R. A. Woods, X. Zheng, R. P. Ibbitt, A. G. Slater, J. Schmidt, and M. J. Uddstrom (2008), Hydrological data assimilation with the ensemble Kalman filter: Use of streamflow observations to update states in a distributed hydrological model, *Adv Water Resour*, *31*(10), 1309-1324.

Crow, W., and D. Ryu (2009), A new data assimilation approach for improving runoff prediction using remotely-sensed soil moisture retrievals, *Hydrology and Earth System Sciences*, *13*(1), 1.

Crow, W., R. Bindlish, and T. Jackson (2005), The added value of spaceborne passive microwave soil moisture retrievals for forecasting rainfall-runoff partitioning, *Geophysical Research Letters*, *32*(18).

Duan, Q., S. Sorooshian, and V. K. Gupta (1994), Optimal use of the SCE-UA global optimization method for calibrating watershed models, *Journal of Hydrology*, *158*(3–4), 265-284.

Gao, H., E. F. Wood, M. Drusch, and M. F. McCabe (2007), Copula-derived observation operators for assimilating TMI and AMSR-E retrieved soil moisture into land surface models, *Journal of Hydrometeorology*, *8*(3), 413-429.

Hong, Y., K. L. Hsu, S. Sorooshian, and X. G. Gao (2004), Precipitation Estimation from Remotely Sensed Imagery using an Artificial Neural Network Cloud Classification System, *J Appl Meteorol*, *43*(12), 1834-1852.

Huffman, G. J., D. T. Bolvin, E. J. Nelkin, D. B. Wolff, R. F. Adler, G. Gu, Y. Hong, K. P. Bowman, and E. F. Stocker (2007), The TRMM Multisatellite Precipitation Analysis (TMPA): Quasi-Global, Multiyear, Combined-Sensor Precipitation Estimates at Fine Scales, *Journal of Hydrometeorology*, *8*(1), 38-55.

Hughes, D., D. Kingston, and M. Todd (2011), Uncertainty in water resources availability in the Okavango River basin as a result of climate change, *Hydrology and Earth System Sciences*, *15*(3), 931-941.

Hughes, D. A., L. Andersson, J. Wilk, and H. H. Savenije (2006), Regional calibration of the Pitman model for the Okavango River, *Journal of Hydrology*, *331*(1), 30-42.

Joyce, R. J., J. E. Janowiak, P. A. Arkin, and P. P. Xie (2004), CMORPH: A method that produces global precipitation estimates from passive microwave and infrared data at high spatial and temporal resolution, *Journal of Hydrometeorology*, *5*(3), 487-503.

Khan, S. I., H. Yang, H. J. Vergara, J. J. Gourley, G. R. Brakenridge, T. De Groeve, Z. L. Flamig, F. Policelli, and Y. Bin (2012), Microwave Satellite Data for Hydrologic Modeling in Ungauged Basins, *Geoscience and Remote Sensing Letters, IEEE*, *9*(4), 663-667.

Kugler, Z., and T. D. Groeve (2007), The global flood detection system, *JRC Scientific and Technical Reports*, *EUR 23303 EN*

McCarthy, J. M., T. Gumbricht, T. McCarthy, P. Frost, K. Wessels, and F. Seidel (2003), Flooding patterns of the Okavango wetland in Botswana between 1972 and 2000, *AMBIO: A Journal of the Human Environment*, *32*(7), 453-457.

Milzow, C., P. E. Krogh, and P. Bauer-Gottwein (2011), Combining satellite radar altimetry, SAR surface soil moisture and GRACE total storage changes for hydrological model calibration in a large poorly gauged catchment, *Hydrology and Earth System Sciences*, *15*(6), 1729-1743.

Milzow, C., L. Kgotlhang, P. Bauer-Gottwein, P. Meier, and W. Kinzelbach (2009a), Regional review: the hydrology of the Okavango Delta, Botswana—processes, data and modelling, *Hydrogeology Journal*, *17*(6), 1297-1328.

Milzow, C., L. Kgotlhang, W. Kinzelbach, P. Meier, and P. Bauer-Gottwein (2009b), The role of remote sensing in hydrological modelling of the Okavango Delta, Botswana, *Journal of environmental management*, *90*(7), 2252-2260.

Pauwels, V., R. Hoeben, N. E. Verhoest, F. P. De Troch, and P. A. Troch (2002), Improvement of TOPLATS-based discharge predictions through assimilation of ERS-based remotely sensed soil moisture values, *Hydrological Processes*, *16*(5), 995-1013.

Pauwels, V. R., and G. J. De Lannoy (2006), Improvement of modeled soil wetness conditions and turbulent fluxes through the assimilation of observed discharge, *Journal of Hydrometeorology*, *7*(3), 458-477.

Salvia, M., F. Grings, P. Ferrazzoli, V. Barraza, V. Douna, P. Perna, C. Bruscantini, and H. Karszenbaum (2011), Estimating flooded area and mean water level using active and passive microwaves: the example of Parana River Delta floodplain, *Hydrology and Earth System Sciences*, *15*(8), 2679-2692.

Sorooshian, S., K.-L. Hsu, G. XIAOGANG, H. V. Gupta, B. Imam, and D. Braithwaite (2000), Evaluation of PERSIANN system satellite-based estimates of tropical rainfall, *Bulletin of the American Meteorological Society*, *81*(9), 2035-2046.

Temimi, M., R. Leconte, F. Brissette, and N. Chaouch (2007), Flood and soil wetness monitoring over the Mackenzie River Basin using AMSR-E 37 GHz brightness temperature, *Journal of Hydrology*, *333*(2–4), 317-328.

Temimi, M., T. Lacava, T. Lakhankar, V. Tramutoli, H. Ghedira, R. Ata, and R. Khanbilvardi (2011), A multi-temporal analysis of AMSR-E data for flood and discharge monitoring during the 2008 flood in Iowa, *Hydrological Processes*, *25*(16), 2623-2634.

Turk, F. J., and S. D. Miller (2005), Toward improved characterization of remotely sensed precipitation regimes with MODIS/AMSR-E blended data techniques, *Ieee T Geosci Remote*, *43*(5), 1059-1069.

Wang, J., et al. (2011), The coupled routing and excess storage (CREST) distributed hydrological model, *Hydrological sciences journal*, *56*(1), 84-98.

Whitaker, J. S., and T. M. Hamill (2002), Ensemble data assimilation without perturbed observations, *Monthly weather review*, *130*(7), 1913-1924.

List of Figures:

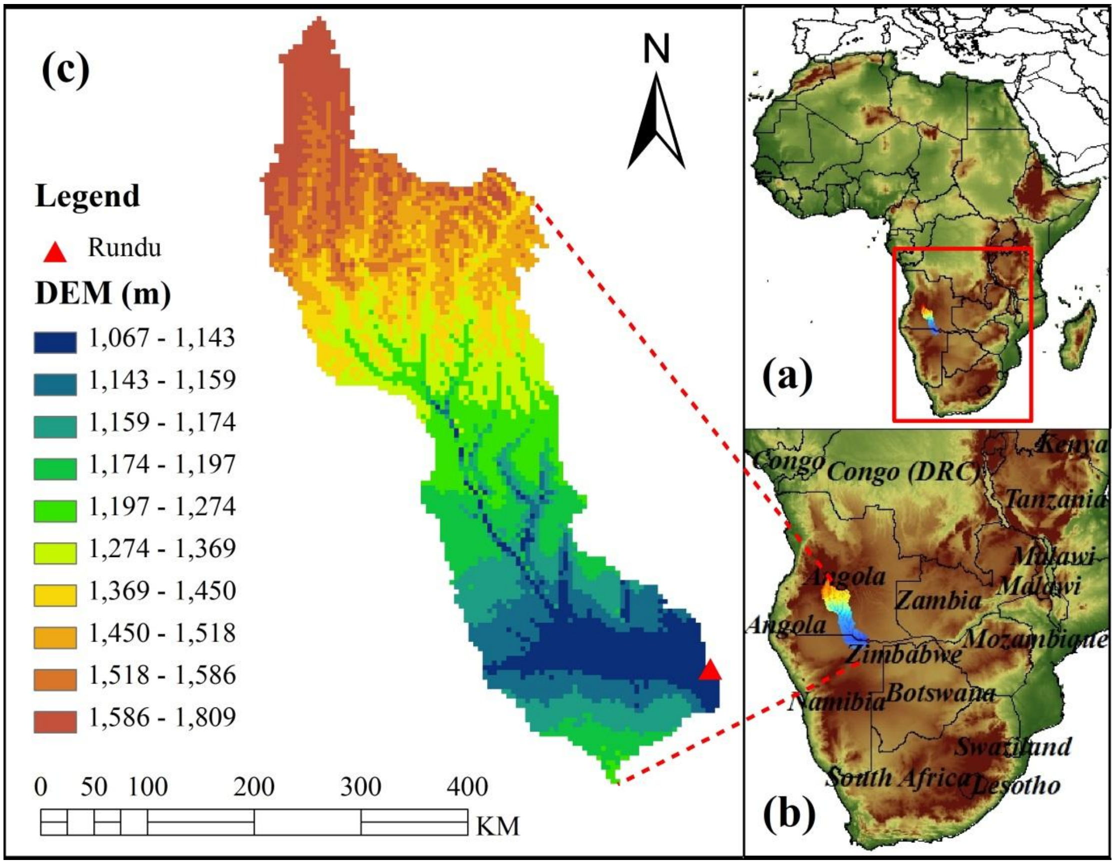

Figure 1. Research Region – Cubango River Basin

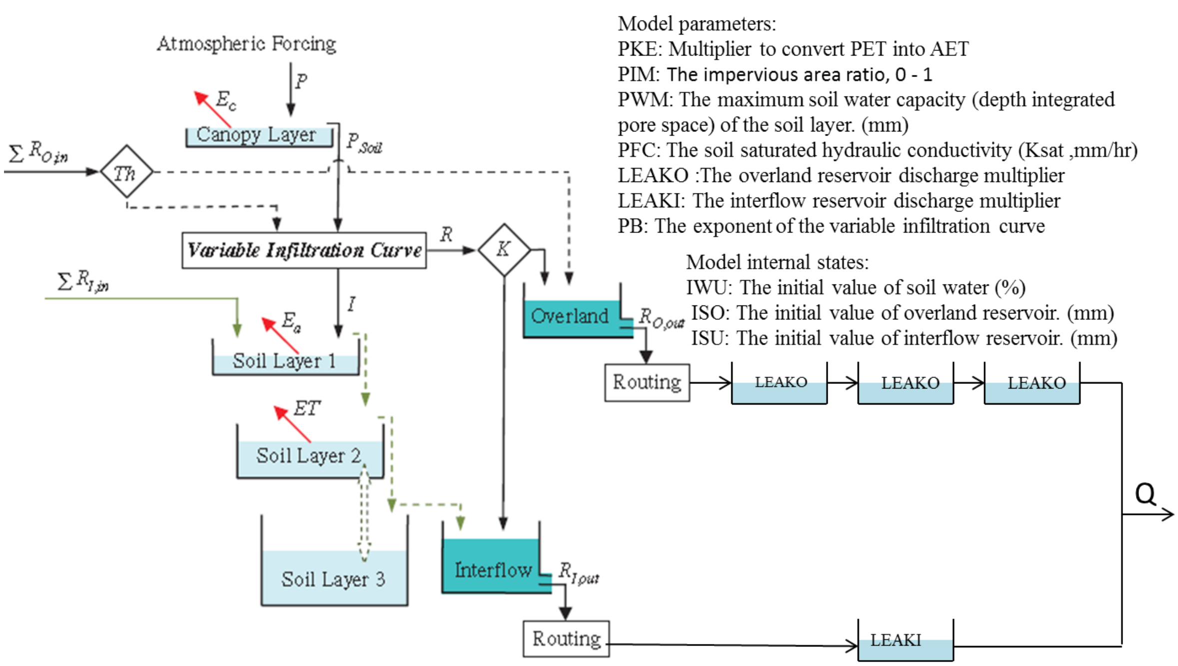

Figure 2. Structure of CREST Model

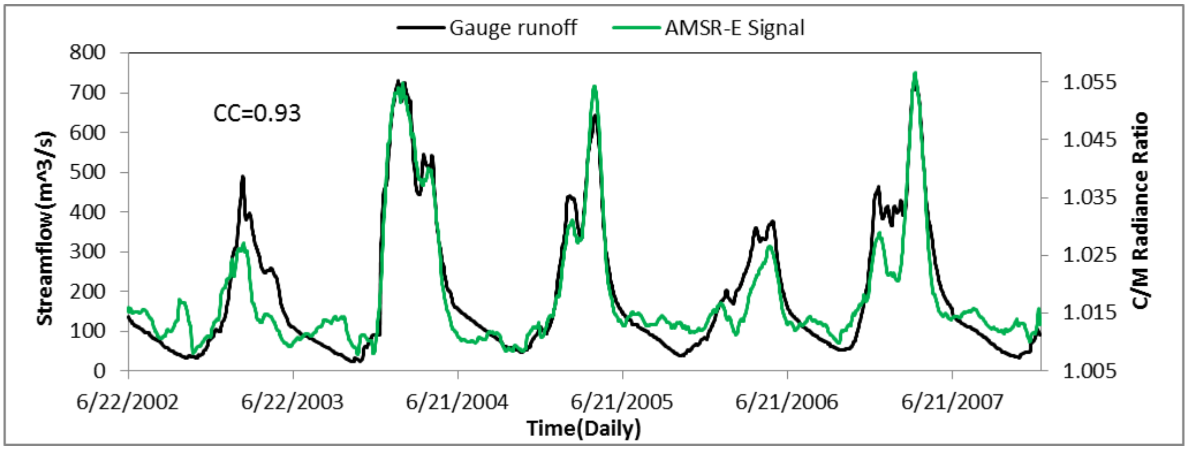

Figure 3. Time series of gauge streamflow observation plotted against primary y-axis and C/M Radiance Ratio plotted against secondary y-axis

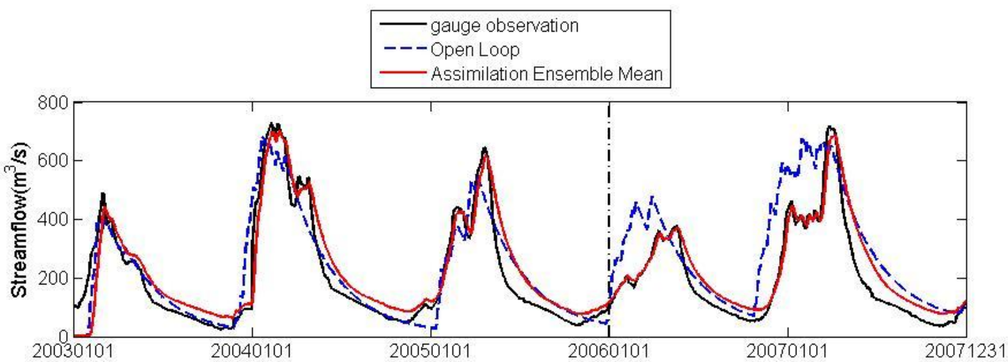

	Calibration		Validation	
	RMSE(%)	NSCE	RMSE(%)	NSCE
Open Loop	34	0.88	64	0.33
Assimilation	29	0.91	27	0.88

Figure 4 Impact of assimilating gauge streamflow into CREST in Experiment 1.

*Note: to the left side of the black dash line is the calibration period from 2003 to 2005; to the right side of the black dash line is the validation period from 2006 to 2007; the same for Figure. 4

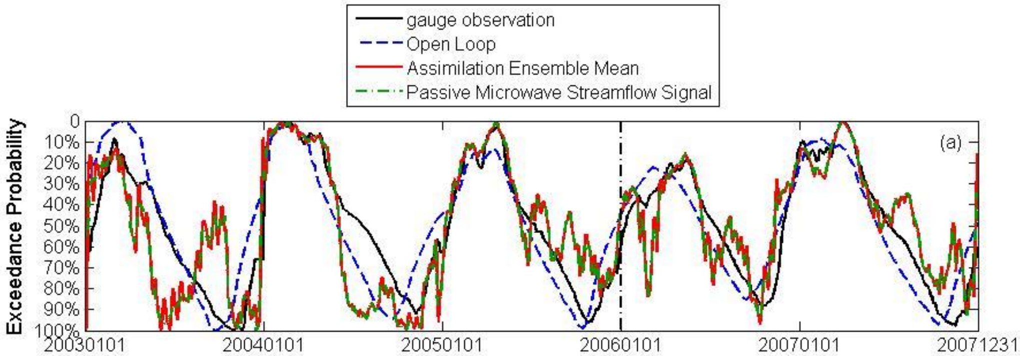

	Calibration		Validation	
	RMSE(%)	NSCE	RMSE(%)	NSCE
Open Loop	27	0.77	25	0.81
Assimilation	36	0.61	31	0.69

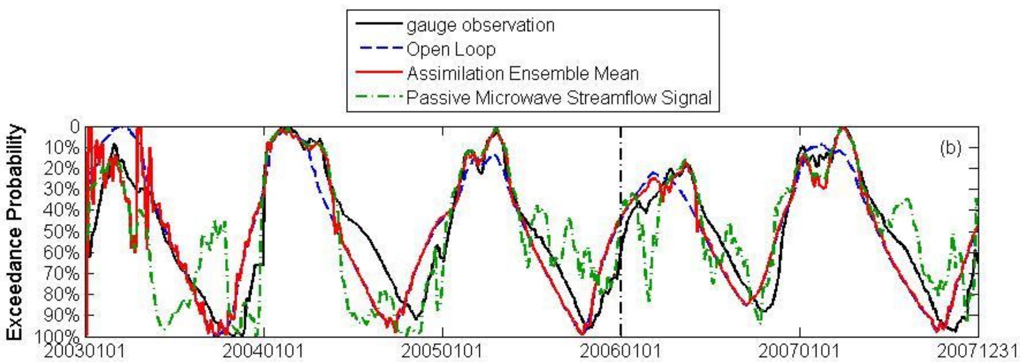

	Calibration		Validation	
	RMSE(%)	NSCE	RMSE(%)	NSCE
Open Loop	27	0.77	25	0.81
Assimilation	26	0.79	23	0.84

Figure 5 Impact of assimilating Passive Microwave signal frequency into CREST in Experiment 2 (a) before threshold and (b) after threshold

442 **List of Tables:**

443 **Table 1.** List of Experiments Design

Exp		Calibration data source	Data Assimilated into Model	Calibration objective function
1		Gauge Streamflow	Gauge Streamflow	Min(RMSE)
2	(a) Before Threshold Applied	AMSR-E Signal Frequency	AMSR-E Signal Frequency	Max(CC)
	(b) After Threshold Applied			

444

445